Supplementary Information

Facile One-Pot Synthesis of Water-Dispersible Phosphate Functionalized Reduced Graphene Oxide Toward High-Performance Energy Storage Devices

Nicolas R. Tanguy, Jeanne N'Diaye, Mohammad Arjmand, Keryn Lian, and Ning Yan*

Materials and Methods

Graphene oxide nanosheets and phosphoric acid (85% in H_2O) were purchased from Sigma-Aldrich and used as received. Deionized water was used to react graphene nanosheets. Synthesis of rGO and P-rGO nanosheets. rGO nanosheets were prepared via hydrothermal dehydration, based on a procedure previously reported.[1] Graphene oxide nanosheets were combined with deionized water (312.5 mL, 0.5 mg/mL) and sonicated for 90 min. P-rGO nanosheets were prepared by inserting 37.5 mL of phosphoric acid in the reaction medium. The final concentration of GO was adjusted to 0.5 mg/mL via addition of deionized water. The dispersion was mixed for 30 min in a 500 mL Teflon-lined stainless-steel vessel. The products were reacted at 180°C for 5 hours. The reactor was then rapidly cooled down to room temperature. The reacted graphene nanosheets were filtered, washed and centrifuged with excess deionized water to remove by-products, before re-dispersing in deionized water and sonicating for 60 min. Several other batches of P-rGO were prepared in a 40 mL Teflon lined autoclave while keeping similar weight ratio of water, phosphoric acid and graphene. These batches were used for X-ray Photoelectron Spectroscopy (XPS), Nuclear Magnetic Resonance (NMR), X-Ray Diffraction (XRD), conductivity and UV-Vis characterization. The rGO and P-rGO dispersions were first frozen in liquid N_2 before being placed in a freeze-dryer for one week to obtain a final porous solid and kept for electrochemical measurements.

Characterization

XPS was used to determine the atomic composition of the graphene nanosheets and of the carbon tape. The nanosheets were deposited onto double-sided C-tape and then analyzed. XPS spectra were collected on a Thermofisher Scientific K-Alpha XPS spectrometer (Thermofisher Scientific, E. Grinstead, UK) using a monochromatic Al Kα X-rays with a nominal spot size of 400 μm diameter. An e/Ar+ floodgun, supplied with the equipment, was used for charge compensation. Each sample was subjected to a survey spectrum with a low energy resolution (pass energy – 150 eV), where only C, O and P were detected. Then, high resolution (pass energy – 25 eV) spectra were recorded for C1s, O1s, and P2p regions. Relative atomic % was calculated from these peaks employing the sensitivity factors provided with the instrument (C1s – 1; O1s – 2.881; P2p – 1.353). Peak fitting was carried out on these regions with a Lorentzian/Gaussian mix of 30%. With the exception of the main peak, assigned to sp2-C, symmetric peak shapes were used. All instrument operation and data processing were accomplished with the Avantage v. 5.962 software supplied with the instrument. Surface characteristics of GO, rGO and P-rGO were investigated via zeta potential analysis (Zeta Plus, Brookhaven Instrument Corporation, USA). A few mg of graphene nanosheets were dispersed in 20 mL of deionized water and the zeta potential was calculated as an average of 10 measurements. Mixtures were sonicated for 5 min and left standing 30 min prior to testing. The morphology of graphene nanosheets and energy dispersive X-ray spectra of the graphene nanosheets were evaluated using transmission electron microscopy (TEM) (JEOL 2010 HRTEM, Japan). Dispersion of P-rGO (0.05 mg/mL) in water was sonicated for 1 hour before drop-casting one drop on a copper grid for TEM. Energy dispersive X-ray spectra were acquired on 10 layers of 1 mL of P-rGO suspension (0.1 mg/mL) drop-casted and dried at 80°C on a spare

part of a silicon wafer. The thermal stability was determined by placing 10 μL of suspension in a TGA pan using a thermal gravimetric analyzer (TGA, TA TGA-Q500, TA Instruments, USA) under air. The samples were first dried to 105°C for 10 min before a ramp at 10°C/min until to 800°C. X-ray diffraction pattern of the graphene nanosheets was obtained using a Philips (PW1830) diffractometer (40 kV, 40 mA, Netherlands). Experiments were conducted using Cu Kα (λ=15.4 nm) with a Ni filter. The nanosheets diffraction patterns were recorded from 5° to 50° with an increment of 0.02° and 2 sec per step. 10 layers of 1 mL of GO, rGO or P-rGO suspension (0.1 mg/mL) were drop-casted and dried at 80°C on a zero-background slide. Raman spectra were acquired at laser excitation wavelength of 532 nm and equipped with a nitrogen cooled charge coupled device detector (Senterra Raman Microscope, Bruker, USA), which was used to find band positions, correct baseline, and normalize the results. I_D/I_G averages, band positions and respective standard deviation were calculated based on three or four Raman spectra of each nanomaterial. 1 mL of GO, rGO and P-rGO dispersion, at concentration of 0.5 mg/mL was drop casted and dried at 80°C on glass slides. The procedure was repeated five times to ensure sufficient thickness.

UV-Vis absorbance spectra of the graphene nanosheets were tested on a diode array UV–Vis spectrophotometer (Ocean Optics Inc., USB4000, USA) coupled with a temperature-controlled holder (Quantum Northwest Inc., USA). Dispersions of GO, rGO and P-rGO were prepared at concentration of 0.05 mg/mL, sonicated for 30 min and allowed to stabilize for 1 hour before being placed in the UV-Vis cuvette. UV-Vis spectra were acquired at 25°C over 200-800 nm range with 1 nm data interval and 600 nm/min and deionized water was used as baseline. 1D ^{31}P solid state MAS spectra were acquired using an Agilent DD2 spectrometer (Agilent Technologies Inc., Santa Clara, CA) equipped with a 3.2mm BioMAS probe with sample spinning set to 3000 Hz. Spectra were acquired using the standard vendor-supplied Onepul pulse sequence at 25°C over an 83333.3

Hz spectral window, with an 8.0s recycle delay, 6000 transients, and an excitation frequency of 283.384 MHz for ^{31}P. All pulse widths and power levels were adjusted to ensure optimal signal:noise prior to acquiring the ^{31}P MAS spectra. P-rGO dispersion was oven dried overnight at 80°C and packed in the probe. Cyclic voltammetry (CV) was used to study the electrochemical behavior of rGO and P-rGO. All CV profiles were recorded with a Princeton Applied Research VersaSTAT3 potentiostat (Princeton Applied Research, USA). Both materials were tested in a 3-electrode cell in 1M sulfuric acid (H_2SO_4). The dried rGO and P-rGO were grinded into a cavity microelectrode working electrode (CME), which had a volume of 8.19×10^{-6} cm^3.[2] A silver/silver chloride (Ag/AgCl) and a platinum mesh were used as reference and counter electrodes, respectively.). The capacitance in farad (F) was calculated by integrating the charge over the given voltage window from the CV profile using equation 1:

$$C = \frac{\int_{V1}^{V2} i(V)dV}{v\,(V_2 - V_1)} = \frac{\int idt}{\Delta V} = \frac{Q}{\Delta V} \quad (1)$$

Where Q in Coulomb (C) is the charge and ΔV is the voltage window in volt (V). The volumetric capacitance in F/cm3 was obtained by dividing the capacitance by the volume of the cavity microelectrode used as the working electrode.

Note on XPS results

Carbon tape XPS survey and de-convoluted C1s spectra were recorded following the same protocol as used during sample testing, as shown in Figure S2. The carbon tape XPS survey showcased two peaks representing Si2s and Si2p, accounting for Si content of approximatively 4.1%, Figure S2a). In comparison, Si2s and Si2p peaks could not be observed on the XPS survey of GO, rGO and P-rGO, as shown in Figure 1, S1 and S2. In addition, the de-convoluted C1s peak

of the carbon tape demonstrated a different pattern as compared to that of observed for GO, rGO and P-rGO, as shown in Figure 1, S1 and S2c), which corroborated that the use of carbon tape had little to no effect on the XPS results obtained for the samples. Lastly, the XPS survey of the carbon tape did not show a peak related to P atoms in the spectra, as shown in Figure S2d), which indicated that the presence of the P2p peak in the XPS spectra of P-rGO is due to recording the spectra of the deposited sample on the carbon tape.

Acknowledgements

Authors would like to thank NSERC Canada (Discovery Grant RGPIN-2017-06737, Discovery RGPIN-2016-06219 and Strategic grant 2100-120694), and the Fond de Recherche Nature et Technologie du Québec PhD graduate scholarship for the financial support. We thank NSERC discovery grant. We acknowledge the Ontario Centre for the Characterization of Advanced Materials (OCCAM), Department of Chemical Engineering and Applied Chemistry, University of Toronto, Dr. Rana Sodhi and Dr. Peter Brodersen for their help with XPS analysis. We are grateful to Darcy Burns for his help in conducting ^{31}P NMR testings and for devising a methodology and to the CSICOMP NMR Facility. We thank Ms. Samaneh Dordani Haghighi for designing and drawing the graphical abstract and schematics. We would also like to thank Arthur Hendsbee and Prof. Yuning Li for assisting with the conductivity measurements.

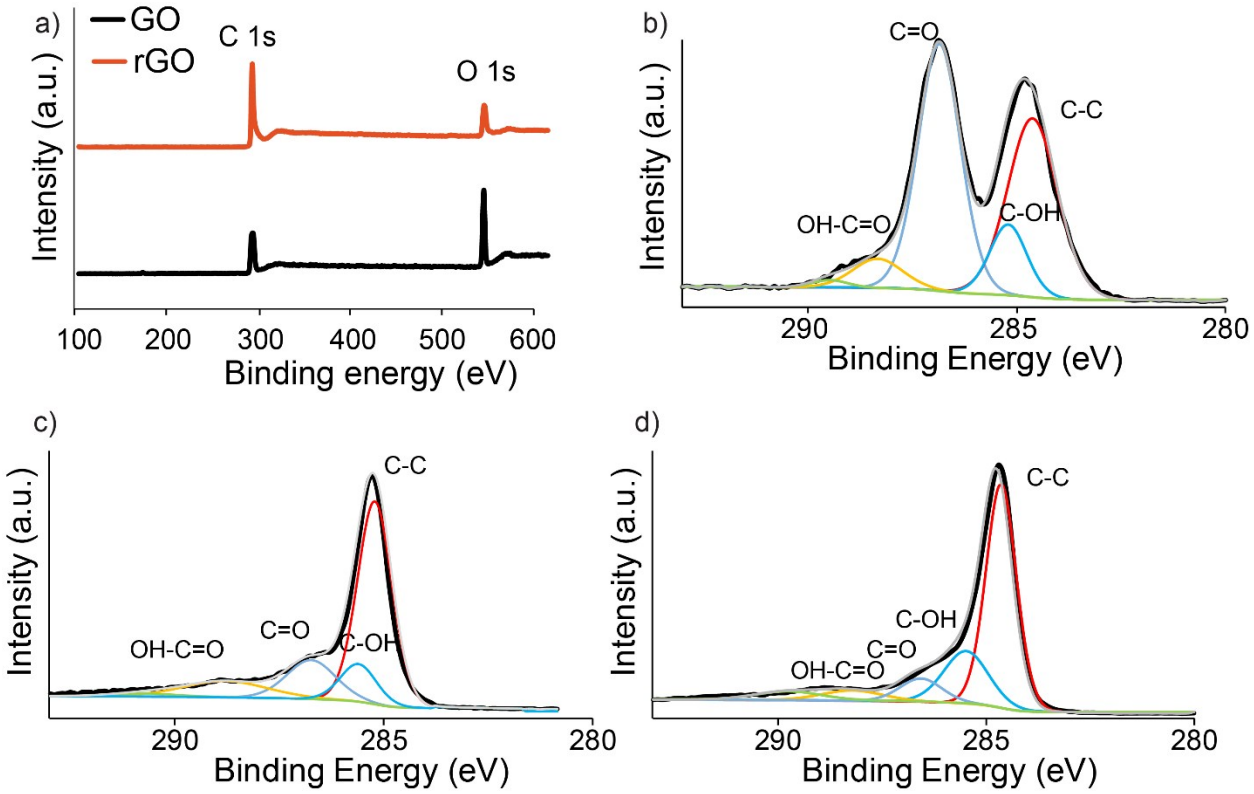

Figure S1. X-Ray photoelectron spectroscopy (XPS) a) survey of GO and rGO and high resolution de-convoluted C1s peak of b) GO, c) rGO and d) P-rGO.

Table S1. X-ray photoelectron spectroscopy (XPS) survey results. Atomic concentration of carbon, oxygen and phosphorus in synthesized nanosheets.

Sample Type	Component	Peak BE (eV)	Atomic Conc. (%)
P-rGO	C	284.52	75.86
	O	532.26	20.95
	P	134.17	3.19
rGO	C	284.48	83.55
	O	531.37	16.45
	P	134.00	-
GO	C	285.29	67.03
	O	531.77	32.97
	P	134.00	-

Table S2. X-ray photoelectron spectroscopy (XPS) peak positions data for C1s line of synthesized nanofillers. Peak C1s was de-convoluted into five diverse segments.

Nanomaterial	Component Assignment	Peak BE (eV)	Atomic Conc. (%)
GO	C-C, C-H	284.62	37.63
	C-OH	285.20	11.04
	C=O	286.85	43.93
	COOH	288.33	6.21
	Satellite	289.47	1.19
RGO	C-C, C-H	284.72	59.17
	C-OH	285.14	11.50
	C=O	286.34	16.03
	OH-C=O	288.52	11.55
	Satellite	290.61	1.75
P-rGO	C-C, C-H	284.70	60.54
	C-OH	285.58	20.46
	C=O	286.67	5.65
	COOH	287.65	8.65
	Satellite	289.85	4.70

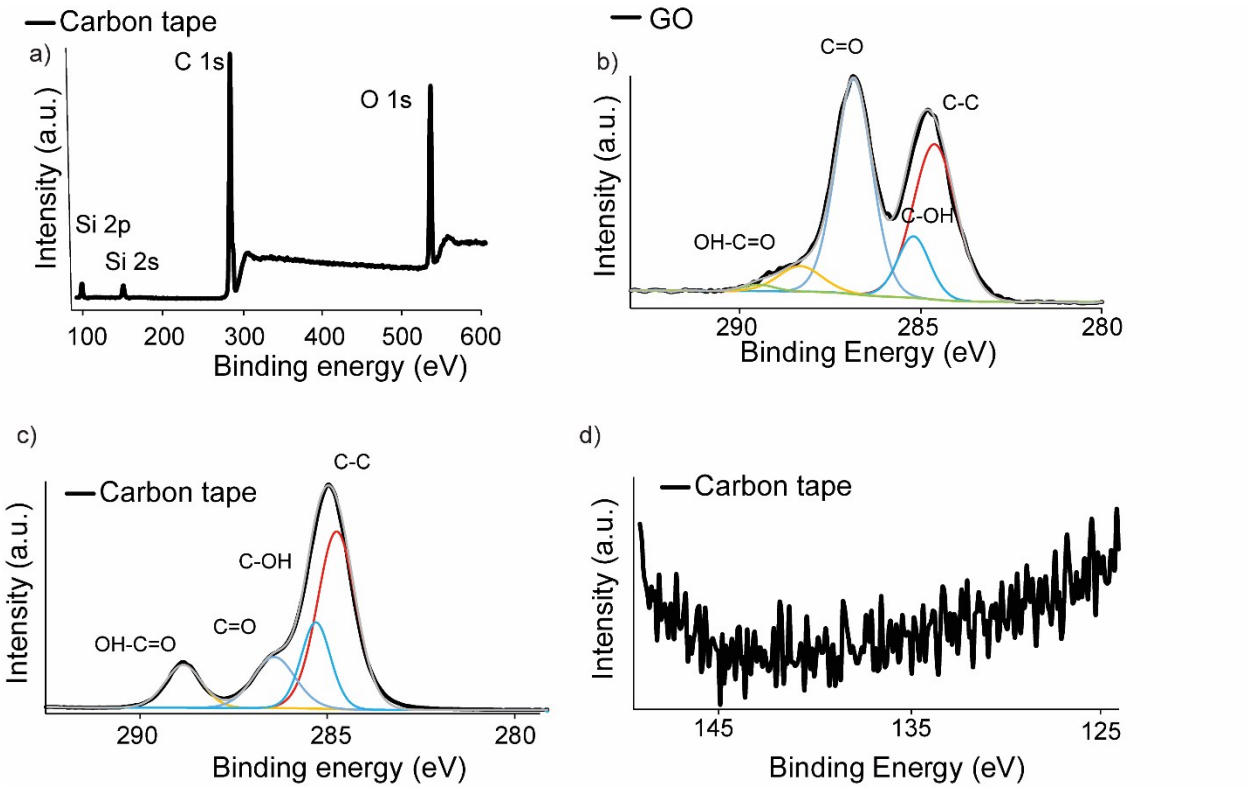

Figure S2. X-Ray photoelectron spectroscopy (XPS) a) survey of carbon tape, high resolution de-convoluted C1s peak of b) GO and c) carbon tape and d) high resolution spectra observed at binding energy representative of P2p peak for carbon tape.

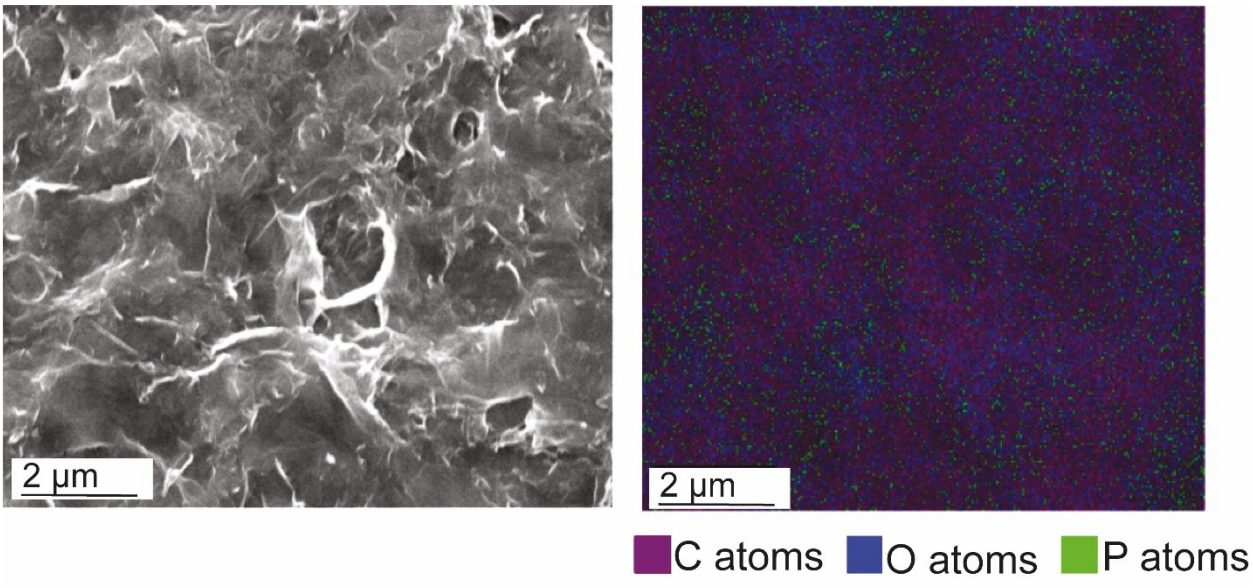

Figure S3. Left side - SEM image and Right side - EDS mapping results of phosphate functionalized reduced graphene oxide film.

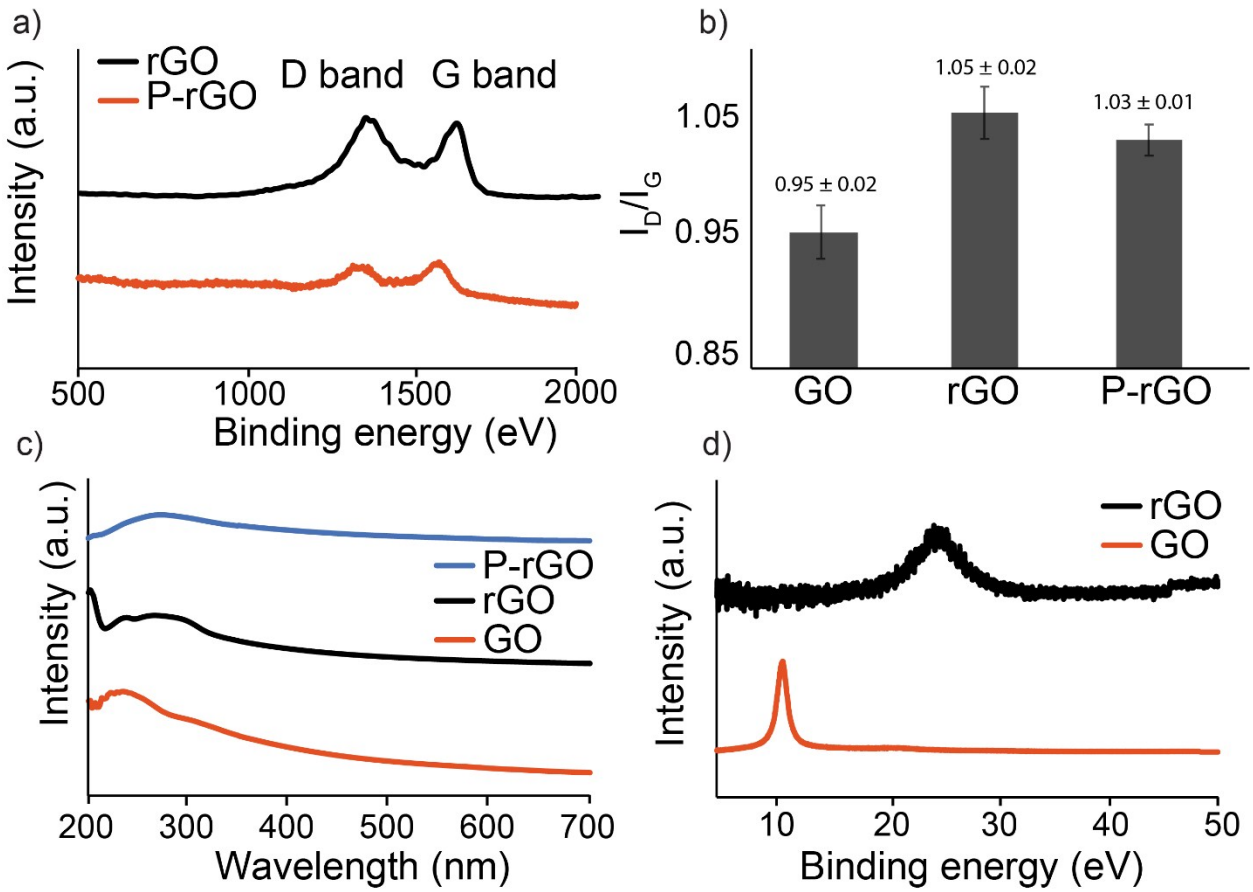

Figure S4. a) Raman spectra of GO and rGO, b) I_D/I_G ratio of GO, rGO and P-rGO, c) UV-Vis spectra of GO, rGO and P-rGO and d) X-Ray diffraction (XRD) pattern of GO and rGO.

Table S3. XRD characteristics of GO, rGO and P-rGO.

	XRD (2θ)	d-spacing (nm)	FWHM	D (nm)	n
GO	10.9	0.8	1.4	5.7	7-8
rGO	24.5	0.4	5.4	1.6	4-5
P-rGO	24.16	0.4	5.5	1.6	4-5

Table S4. Raman shifts, I_D/I_G ratio, UV-Vis adsorption and zeta potential of GO, rGO and P-rGO.

	Raman shift (cm^{-1})			UV-Vis (nm)	Zeta Potential (mV)
	D band	G band	I_D/I_G		
GO	1349±7	1589±4.2	0.95±0.02	235	-39.23 ± 3.00
rGO	1343±2.5	1593±3.3	1.05±0.02	266	-33.79 ± 3.94
P-rGO	1339±2.9	1587±2.6	1.03±0.01	272	10.84 ± 4.66

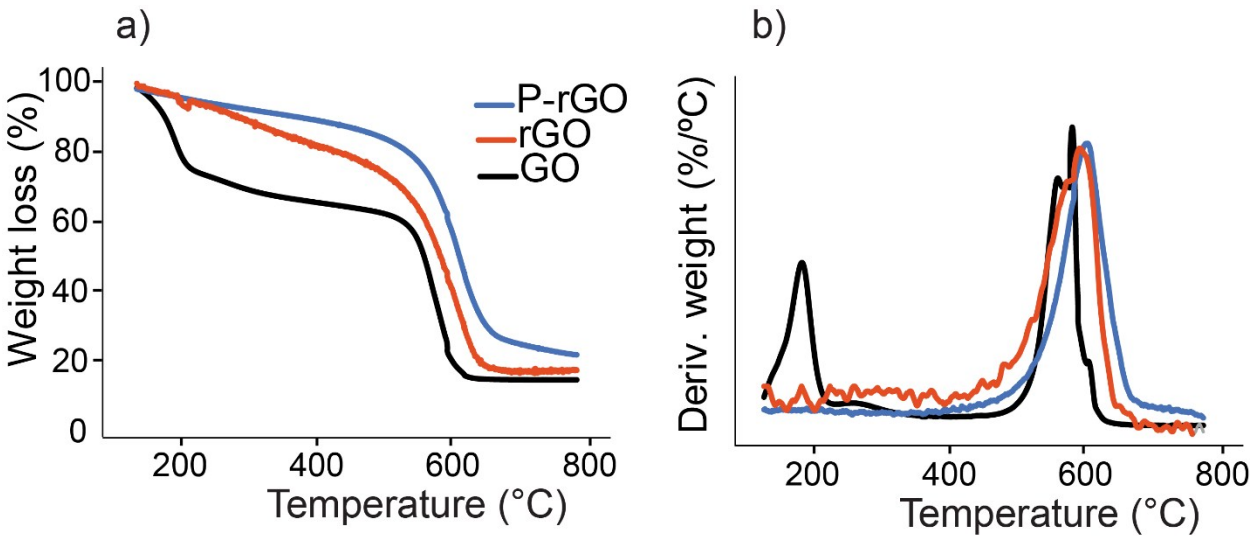

Figure S5. a) TGA thermograph of GO, rGO and P-rGO and b) First derivative thermograph of GO, rGO and P-rGO.

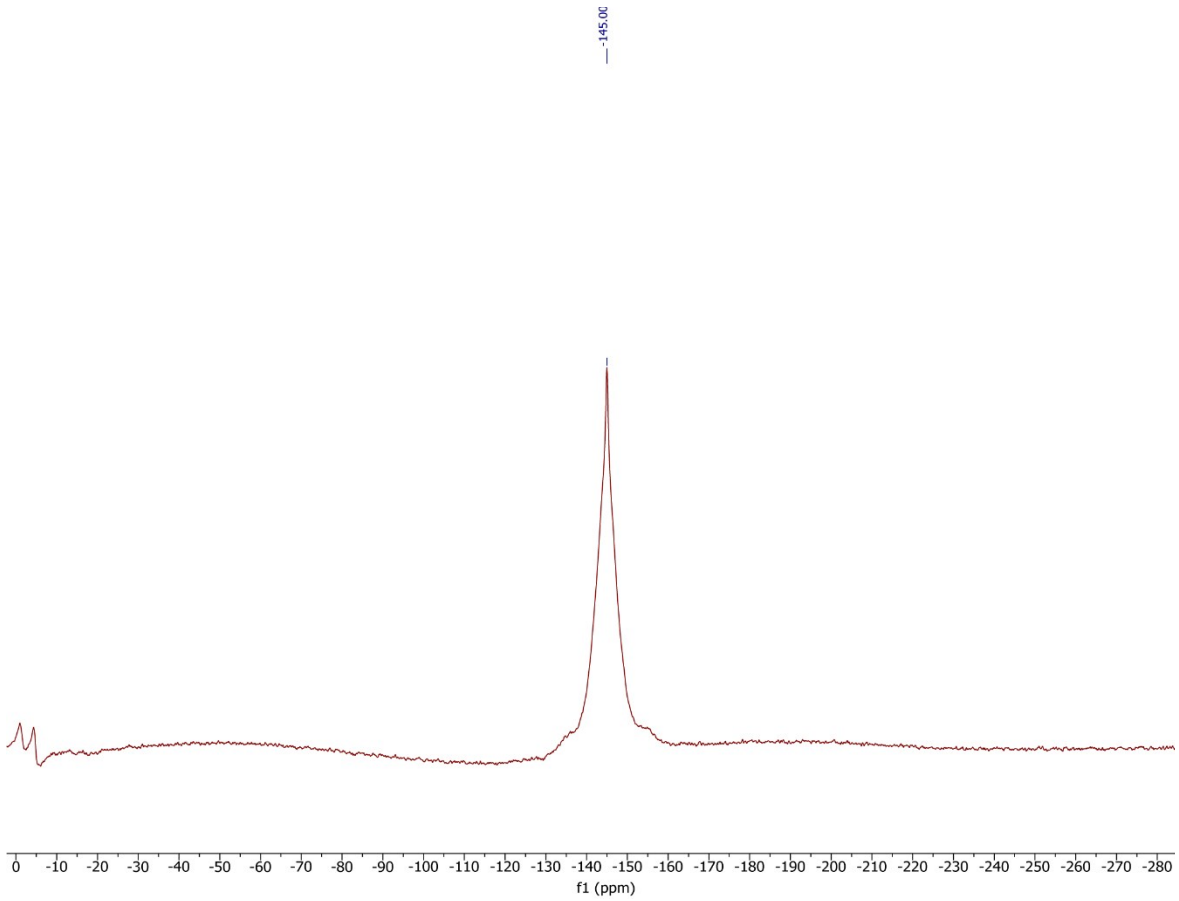

Figure S6. CP/MAS-^{31}P NMR NaPF6 reference.

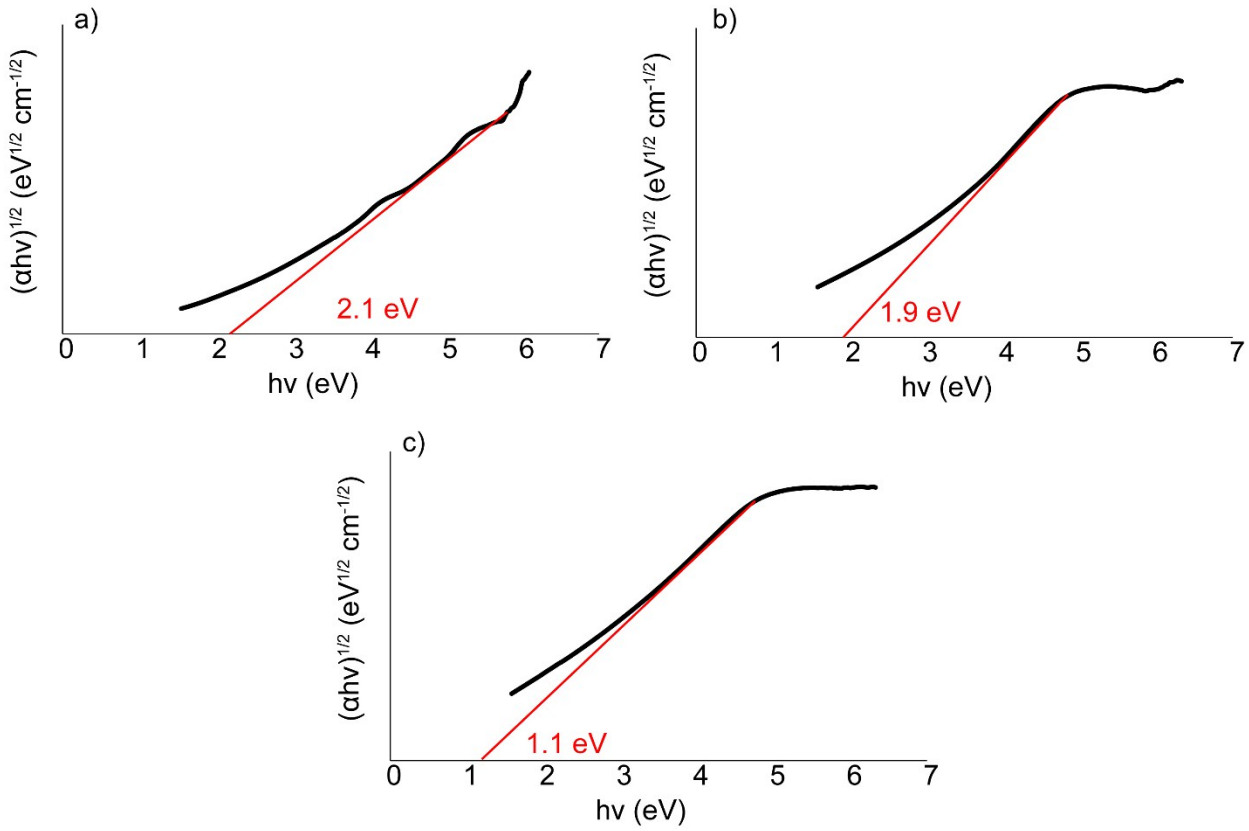

Figure S7. Tauc plot of a) GO, b) rGO and c) P-rGO extracted from UV-Vis spectroscopy results.

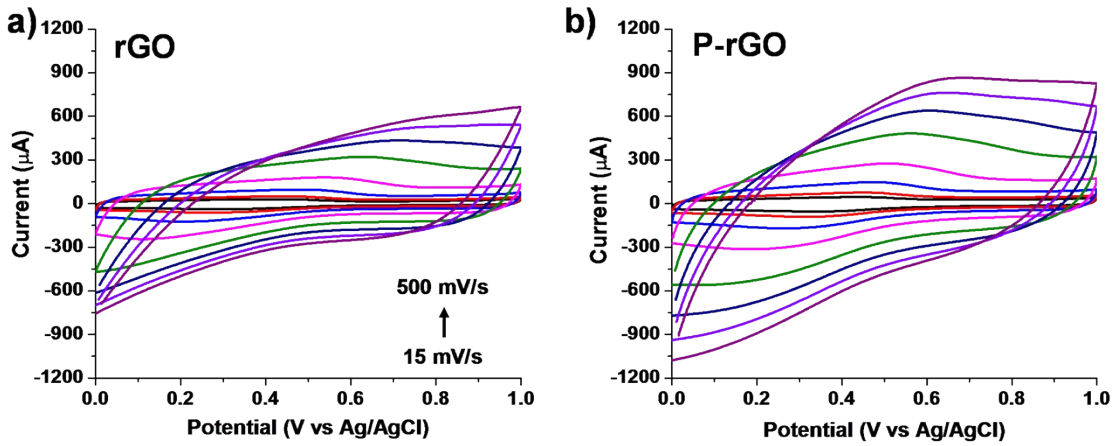

Figure S8. CV profile of a) rGO and b) P-rGO at scan rate between 15 mV/s to 500 mV/s.

Table S5. Comparative table of the volumetric capacitance of graphene-based electrodes for ECs.

Materials	Fabrication method	Electrolyte	Capacitance (F/cm^3)	Ref
Graphene film	Vacuum filtration and capillary compression	1M H_2SO_4	255	[3]
Holey graphene	Thermal activation with H_2O_2	6M KOH	212	[4]
Ultrathin RGO films		1M H_2SO_4-PVA gel	197.3	[5]
rGO	Reduction in the presence of urea	6M KOH	196	[6]
rGO hydrogel	Electrochemical reduction	6M KOH	176.5	[7]
rGO (This study)		1M H_2SO_4	178.8	
P-rGO (This study)	Hydrothermal reduction in the presence of H_3PO_4	1M H_2SO_4	259.7	

Reference

1 Y. Zhou, Q. Bao, L. A. L. Tang, Y. Zhong and K. P. Loh, *Chem. Mater.*, 2009, **21**, 2950–2956.

2 C. Portet, J. Chmiola, Y. Gogotsi, S. Park and K. Lian, *Electrochim. Acta*, 2008, **53**, 7675–7680.

3 X. Yang, C. Cheng, Y. Wang, L. Qiu and D. Li, *Science (80-.).*, 2013, **341**, 534–537.

4 Y. Xu, Z. Lin, X. Zhong, X. Huang, N. O. Weiss, Y. Huang and X. Duan, *Nat. Commun.*, 2014, **5**, 4554.

5 G. F. Wang, H. Qin, X. Gao, Y. Cao, W. Wang, F. C. Wang, H. A. Wu, H. P. Cong and S. H. Yu, *Chem*, 2018, **4**, 896–910.

6 Z. Lei, L. Lu and X. S. Zhao, *Energy Environ. Sci.*, 2012, **5**, 6391–6399.

7 V. H. Pham and J. H. Dickerson, *J. Phys. Chem. C*, 2016, **120**, 5353–5360.